Effects of Solvent Interactions on the Structure and Properties of Prepared PAni Nanofibers

Sujata Pramanik,[1] Niranjan Karak,[1] Somik Banerjee,[2] Ashok Kumar[2]

[1]*Advanced Polymer and Nanomaterial Laboratory, Department of Chemical Sciences, Tezpur University, Tezpur, Assam 784028, India*
[2]*Material Research Laboratory, Department of Physics, Tezpur University, Tezpur, Assam 784028, India*

Received 28 July 2011; accepted 3 February 2012
DOI 10.1002/app.36950
Published online in Wiley Online Library (wileyonlinelibrary.com).

ABSTRACT: The changes of structure and properties of nanofibers were studied as a function of solubility parameters of the organic solvents that are used in interfacial polymerization of polyaniline (PAni) nanofibers. The presence of UV–visible absorbance at 340, 440, and 800 nm confirmed the formation of emeraldine salt structure of the prepared PAni nanofibers. Fourier transform infrared spectral results indicate an increasing trend of benzenoid to quinoid ratio with the decrease of interaction of the solvents with aniline. This can be correlated to the increase in the degree of conjugation of the polymer chain. Photoluminescence study revealed an increase in the density of defect state with the decrease of interaction. Single-line approximation technique was used to analyze the broadening of the most intense X-ray reflection peak corresponding to (110) plane of the nanofibers. The greater the solvent–monomer interaction, the lesser was the domain length and π-stacking of the PAni chains. The study of this interaction is instrumental to precisely control the internal conformation of the PAni nanofibers. © 2012 Wiley Periodicals, Inc. J Appl Polym Sci 000: 000–000, 2012

Key words: polyaniline nanofiber; structure and properties; photoluminescence; FTIR

INTRODUCTION

Among the family of π-conjugated polymers, polyaniline (PAni) carves a unique niche because of its unique properties such as good environmental stability, solubility, and simple acid/base doping/dedoping chemistry. PAni is a promising material for a wide range of applications, namely, anticorrosion coatings,[1] batteries,[2] potentiometric sensors,[3] separation membranes,[4] antistatic coatings,[5] and fluorescent sensing for nucleic acid detection.[6] PAni nanofibers possess similar functionalities as the bulk counterpart; however, the former proves to be a better potential for chemical sensing and water dispersability than the latter.[7]

Recently, scientists have focused attention on one-dimensional PAni nanostructures, such as nanofibers, nanotubes, and nanorods, because of their low dimensional structures, organic nature, and metal-like conductivity.[8] Various strategies have been developed for the synthesis of one-dimensional PAni nanostructures by introducing "structure directing agents," which include surfactants,[9] liquid crystals,[10] polyelectrolytes,[11] nanowire seeds,[12] aniline oligmers,[13] and relatively complex bulky organic dopants[14] during the polymerization process. Jing et al.[15] used ultrasonic synthetic approach to synthesize PAni nanofibers. Li and Wang[16] fabricated chiral PAni nanofibers using an aniline oligomer to accelerate the polymerization reaction. Zhang et al.[17] documented a "nanofiber seeding" method to synthesize bulk quantity of PAni nanofibers in one step. Lu et al.[18] reported the preparation of PAni nanofibers by using a "high-gravity oxidative polymerization" in a rotating packed bed. In addition, Huang et al.[5,19] reported a route to synthesize PAni nanofibers at the organic/inorganic interface. Among these reported approaches, interfacial polymerization developed by Huang and Kaner[9] is the most facile as well as template-free approach to synthesize PAni nanofibers. The interfacial polymerization technique yields high-quality PAni nanofibers. The secondary overgrowth is restricted as the hydrophilic nanofibers move toward the aqueous phase leaving the interface for directional polymerization reaction. The relative ease of interfacial polymerization made it the preferred technique in many fields ranging from microencapsulation of pharmaceutical products to the synthesis of conducting polymers.[20,21] Although

Correspondence to: N. Karak (karakniranjan@yahoo.com).
Contract grant sponsors: The authors express their gratitude and thanks to the research project assistant given by DRL, India, through the grant no. DRL/1047/TC, dated 2nd March, 2011, SAP (UGC), India through grant No. F.3-30/2009(SAP-II) and FIST program-2009 (DST), India through the grant No.SR/FST/CSI-203/209/1 dated 06.05.2010. SAIF, NEHU, Shillong, is acknowledged for TEM imaging.

there is a lot of literature on one-dimensional PAni nanofibers including morphological study[22] and structural characterization,[23] studies focusing on the effects of solvent interaction with aniline on the structure and properties of PAni nanofibers synthesized using interfacial polymerization are scanty. Therefore, in this study, the effect of interactions between the monomer (aniline) and different organic solvents used in polymerization process of varying solubility parameter on the structure and properties of PAni nanofibers are explored.

EXPERIMENTAL

Materials

Aniline ($C_6H_5NH_2$) was purchased from Merck (India). It was purified by vacuum distillation in the presence of zinc dust (atomic weight 65.37 g/mol; S.D. Fine-Chem, India) before use. The solvents like butanol (C_4H_4OH, with boiling point of 118°C and density of 0.81 g/cm^3), benzene (C_6H_6, with boiling point of 80°C and density of 0.88 g/cm^3), carbon tetrachloride (CCl_4, with boiling point of 78°C and density of 1.594 g/cm^3), and dichloromethane (CH_2Cl_2, with boiling point of 40°C and density of 1.32 g/cm^3) were distilled before use. Ammonium peroxydisulfate [$(NH_4)_2S_2O_8$] and hydrochloric acid (HCl; 36.46 g/mol, 11.6*N*) were used as purchased (Merck).

Preparation of PAni nanofibers by interfacial polymerization technique

The oxidant, ammonium peroxydisulfate (2.852 g, 0.25*M*), and the dopant, hydrochloric acid (1.54 mL, 1*M*), were dissolved in doubled distilled water (50 mL) in a 100-mL glass vial. In a separate glass vial, distilled aniline (4.56 mL, 1*M*; aniline/oxidant ratio is kept at 4 : 1) was dissolved in 50 mL of the organic solvent. For the denser organic solvents such as carbon tetrachloride and dichloromethane, the aqueous solution of the oxidant and the dopant was carefully added. In the case of the lighter solvents such as 1-butanol and benzene, aniline dissolved in the organic solvent was carefully added to the aqueous solution of the oxidant and the dopant. The PAni nanofibers were formed by keeping the combined system for 12–24 h under a static condition at room temperature. The mass of PAni nanofibers formed gets dispersed in the aqueous phase, which were then centrifuged and washed with double-distilled water followed by methanol for several times until the filtrate became colorless. The product was finally dried in a vacuum oven at 40°C for 28 h.

Characterization

The samples for UV–visible spectroscopy (UV-1700 PharmaSpec spectrophotometer from Shimadzu, Japan) were prepared by dispersing small amount of PAni nanofibers in double-distilled water. All the spectra were recorded between 200 and 900 nm in differential scanning mode using water as the reference. The Fourier transform infrared (FTIR) spectra were recorded on a Nicolet FTIR Impact 410 spectrometer. The samples for FTIR were prepared as pellets by pressing a mixture of PAni and potassium bromide. The wide-angle diffractograms of the fine powdered PAni samples were measured with a scanning rate of 0.05 min^{-1} over a wide scanning angle of $2\theta = 10°–70°$ using Cu Kα radiation by a Rigaku X-ray diffractometer (Miniflex, UK). Photoluminescence (PL) spectra of the samples were acquired using a Perkin-Elmer Ls-55 florescence spectrometer. The samples for conductivity measurements were prepared by pressing them into pellets of 1 cm diameter and analyzed using a Keithley 2400 C source meter. The morphology of the PAni nanofibers was studied using a JEOL JEM 100 CX-transmission electron microscope (TEM) at an operating voltage of 100 kV after casting on carbon-coated copper grids.

RESULTS AND DISCUSSION

The PAni nanofibers prepared using different organic solvents, namely, dichloromethane, 1-butanol, benzene, and carbon tetrachloride (with varying solubility parameters)[24] have been coded as P1, P2, P3, and P4, respectively. The period from the addition of the two aqueous/organic biphasic systems to the beginning of the formation of PAni nanofibers at the interface of the two solvent systems is termed as "induction time" to observe the difference of the polymerization of aniline in different organic solvents. The induction time for the polymerization of aniline dissolved in dichloromethane, 1-butanol, benzene, and carbon tetrachloride was 90, 75, 60, and 30 s, respectively, as given in Table I. In dichloromethane and 1-butanol, the interaction between solvent and aniline molecules inhibits the fast release of the aniline into the interface (because close solubility parameters) and thus retards their interaction with the oxidant and the dopant. This results in longer induction time in dichloromethane and 1-butanol when compared with carbon tetrachloride, as the difference in solubility parameter with respect to aniline is comparatively high in this case. Although the difference in the solubility parameter is same in the case of 1-butanol and benzene, the induction period of the former is more when compared with the latter owing to the polar–polar and hydrogen-bonding

TABLE I
Physical Properties and Interactions of the Organic Solvents and Induction Time for the Formation of PAni Nanofibers

Solvent	Solubility parameter (δ_s) $(cal/cm^3)^{1/2}$	$\delta_a^* - \delta_s$ $(cal/cm^3)^{1/2}$	Dielectric constant	Dipole moment (D)	Induction period (s)	Quantum yield
CH_2Cl_2	9.7	0.6	9.1	1.60	90	0.24
C_4H_9OH	11.4	1.1	17.8	1.66	75	0.13
C_6H_6	9.2	1.1	2.3	0	60	0.11
CCl_4	8.6	1.7	2.2	0	30	0.08

δ_a^* (solubility parameter of aniline) = 10.3 $(cal/cm^3)^{1/2}$.

interactions of the former with the aniline monomer. The smaller difference in the solubility parameter between dichloromethane and aniline when compared with 1-butanol indicates that they have similar internal energies and hence greater interaction. In the case of PAni prepared in benzene and carbon tetrachloride as organic phase, only dispersive interactions exist between them and aniline because of their nonpolar nature. The difference in the induction time may be originated from the difference in intermolecular interaction between the organic solvent and the aniline molecules. Stronger interaction resulted in a longer induction time.

Figure 1 shows the UV–visible spectra of PAni nanofibers synthesized using different organic solvents. The spectra of nanofiber samples contained all of the characteristic peaks of doped form of PAni emeraldine salt. The three absorption bands of nanofibers[25] appeared at around 340 nm corresponding to π–π* transition, a band centered at around 440 nm corresponding to polaron–π* transition and a broad band at around 800 nm assigned to the π–polaron transition. A broad absorption band observed at around 3700 to 1800 cm^{-1} is characteristic of electrically conductive polymers, which reflects the electronic transition from the valence to the conduction band.[26] The UV–visible spectra of PAni nanofibers reveal the existence of a single broad polaronic band deep in the band gap of the PAni, which is stabilized by the Columbic interactions, dielectric screening, and local disorder in the PAni lattice.[27]

TEM micrographs (Fig. 2) exhibit the nanofibrillar morphology of PAni with average diameter around 25–30 nm.[19] Even though the changes in the internal morphology of the PAni nanofibers are not noticeable in electron microscopy images, the changes are revealed from the FTIR, XRD, PL, and conductivity results.

The FTIR spectra of the samples showing the characteristic bands of PAni in the range 500–4000 cm^{-1} are shown in Figure 3. The FTIR bands at around 3435, 1300, and 1150 cm^{-1} are assigned to N—H, C—N, and C=N stretching vibrations, respectively. The strong band at 1150 cm^{-1} is ascribed as a measure of the degree of delocalization of electrons, a characteristic band of conducting PAni nanofibers.[28] The characteristic bands at 1490 and 1576 cm^{-1} are assigned to the benzenoid and quinoid rings,[29] respectively, and were deconvoluted computationally (Fig. 4). The strong absorption band at 1576 cm^{-1} also corresponds to the coupling of the N—H bending and C—N stretching vibrations in PAni nanofibers. It was observed that greater the interaction (i.e., smaller difference in solubility parameter) of the solvent with the monomer, the lesser is the benzenoid to quinoid ratio. Table II shows the values of the band position, intensity, and full width half maximum of the band corresponding to the benzenoid and the quinoid units. Although both 1-butanol and benzene have the same difference in the solubility parameter to aniline, the former has lower benzenoid to quinoid ratio, which can be ascribed to the additional polar–polar interaction of the former with the aniline monomer.

The XRD patterns of different PAni nanofibers (Fig. 5) display broad reflections at around $2\theta = 19.2^\circ$ and 26°, typical of HCl-doped PAni.[30] The peaks at 19.2° and 26° due to the (100) and (110) reflections are assigned to the regular spacing between phenyl rings of adjacent chains of PAni in a

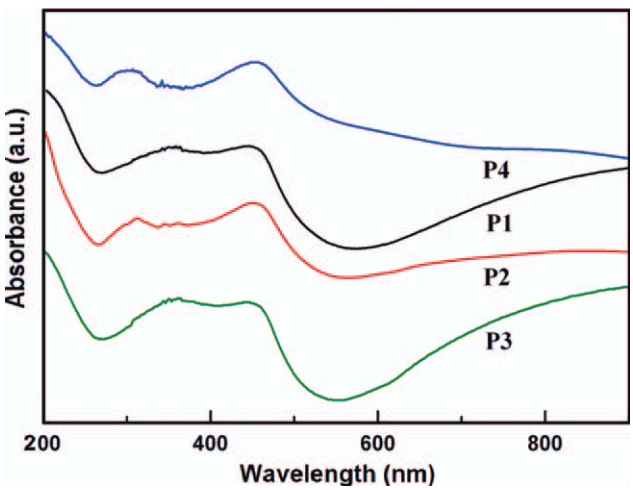

Figure 1 UV–visible spectra of P1, P2, P3, and P4 PAni nanofibers. [Color figure can be viewed in the online issue, which is available at wileyonlinelibrary.com.]

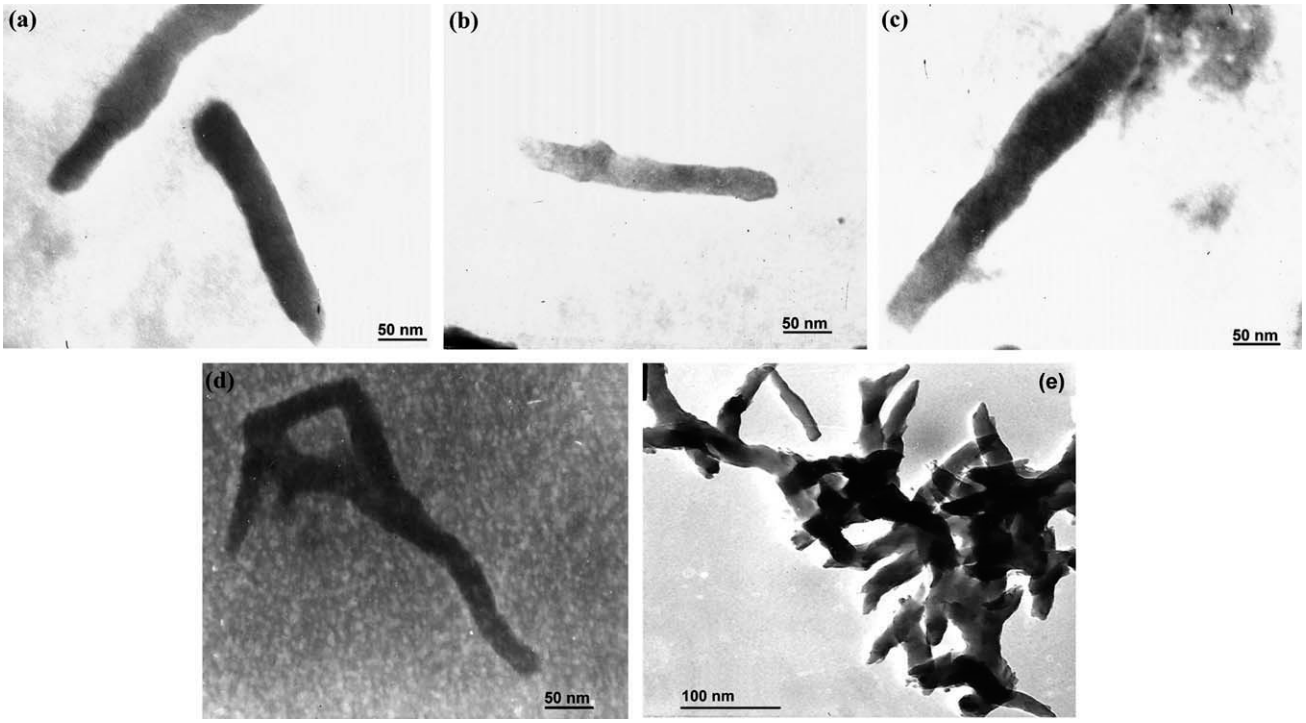

Figure 2 TEM images of (a) P1, (b) P2, (c) P3, (d) P4 PAni nanofibers, and (e) low magnification of P4 PAni nanofibers.

parallel orientation and perpendicular orientation, respectively. A single-line method using a Voigt function has been used to analyze the origin of line broadening in the X-ray diffraction pattern.[27] The more intense (110) reflection peak at about 26° has been deconvoluted computationally (Fig. 6) to calculate the *d*-spacing, domain length, and strain produced in the PAni chains. Line broadening in the X-ray spectra may be due to variation in size of the crystalline domains and strain in the material. The size of coherent domains (or incoherently diffracting domains) is not only limited to the grains but may also include effects of stacking and twin faults and subgrain structures such as small-angle boundaries. The strain broadening, on the other hand, is caused by any lattice imperfection (dislocations and different point defects). The theory is quite general and has been successfully applied to all forms of materials, including oxides and polymers.[31] Thus,

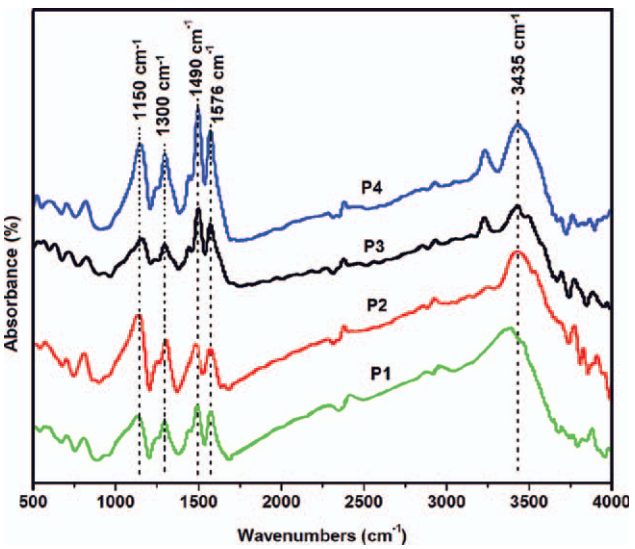

Figure 3 FTIR spectra of P1, P2, P3, and P4 PAni nanofibers showing the characteristic bands in the range 500–4000 cm^{-1}. [Color figure can be viewed in the online issue, which is available at wileyonlinelibrary.com.]

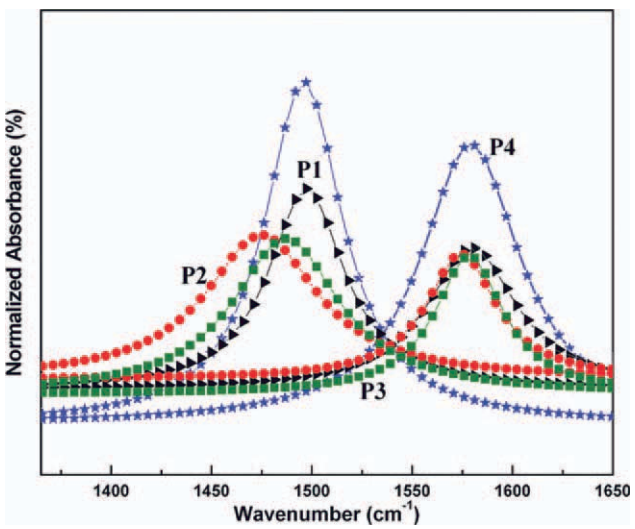

Figure 4 Deconvoluted FTIR peaks of benzenoid and quinoid structures for P1, P2, P3, and P4 PAni nanofibers. [Color figure can be viewed in the online issue, which is available at wileyonlinelibrary.com.]

TABLE II
Deconvolution of the C=C Stretching Vibration of FTIR Peaks Corresponding to the Benzenoid and Quinoid Structures for Different PAni Nanofiber Samples

Sample code	Deconvolution of benzenoid peak (1490 cm^{-1})	Deconvolution of quinoid peak (1576 cm^{-1})
Position		
P1	1487.6	1579.1
P2	1474.3	1577.2
P3	1497.3	1580.5
P4	1495.9	1579.3
Intensity		
P1	11.48	10.42
P2	11.36	10.70
P3	14.76	10.58
P4	25.13	20.59
Full width half maximum		
P1	62.76	46.36
P2	75.50	61.50
P3	45.40	58.82
P4	47.42	61.32

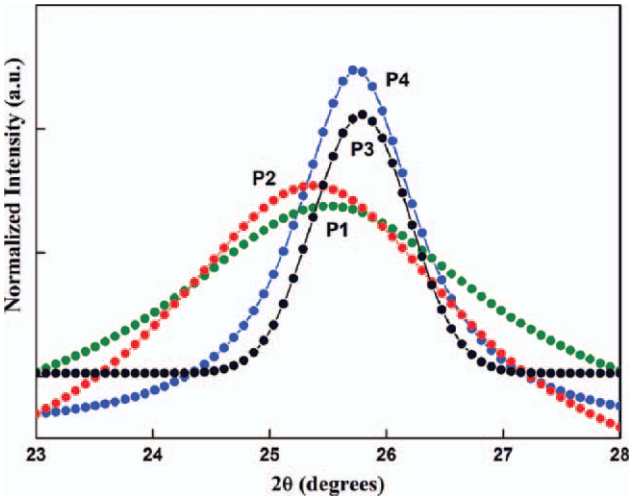

Figure 6 Comparison of diffraction peak corresponding to the (110) plane of P1, P2, P3, and P4 PAni nanofibers. [Color figure can be viewed in the online issue, which is available at wileyonlinelibrary.com.]

investigation of the domain length and strain can provide important insight into the effect of solvent interactions to the structural properties of PAni nanofibers.

It has been observed that with increasing interaction between the solvent and the monomer, the *d*-spacing between the polymer chains increases. The increase in the *d*-spacing from 3.45 Å, in the case of P4, to 3.53 Å in P1 suggests an increase in the angle at which the chains tilt with respect to the (*a*, *b*) basal plane of PAni nanofibers.[27] The increase in the tilt angle of C_{ring}—N—C_{ring} indicates reduction in π-stacking among the PAni chains. Moreover, the contributions of domain length and strain toward the line broadening of the X-ray diffraction pattern have been calculated and summarized in Table III. The

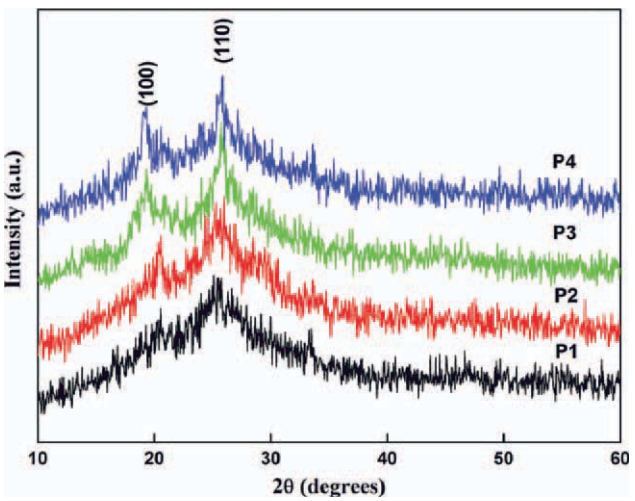

Figure 5 X-ray diffractograms of P1, P2, P3, and P4 PAni nanofibers. [Color figure can be viewed in the online issue, which is available at wileyonlinelibrary.com.]

domain length or the range of order in polymer has also been found to decrease with the increase in the interaction between the organic solvent with aniline. Table III shows that the strain corresponding to the (110) reflection increases from P4 to P1. This can be interpreted as an increase in the concentration of defects within the polymeric backbone of PAni nanofibers. Thus, the broadening of the (110) reflection is attributed to the decrease in the domain length along with the increasing strain in the PAni nanofibers. The lesser the solvent–aniline interaction, the greater is the π-stacking of the PAni chains and the degree of conjugation, which is also evident from the FTIR results.

The PL spectra of different PAni samples are shown in Figure 7. The nanofibers were excited at 220 nm, and they showed luminescence in the blue region of the spectrum around 390 nm.[30] It was observed that PL intensity was quenched with the increase of interaction between the solvent and aniline. The quantum yields of PAni nanofibers were determined using quinine sulfate as the reference. The quantum yields of the PAni nanofibers have been found to decrease from P4 to P1 as 0.24 to 0.08

TABLE III
Solubility Parameter, *d*-spacing, Domain Length (*L*), Strain, and Conductivity of P1, P2, P3, and P4 Samples

Sample	*d*-spacing (Å)	*L* (Å)	Strain (ε) (%)	Conductivity (S/cm)
P1	3.53	19.01	2.3	4.62×10^{-4}
P2	3.49	21.70	1.6	9.62×10^{-4}
P3	3.48	22.77	0.68	1.42×10^{-3}
P4	3.45	81.08	0.26	3.24×10^{-3}

(shown in Table I). This is indicative of the fact that the density of defect states decreases with the increase of interaction.[32] This is further vouched by the characteristic current–voltage (*I–V*) plots of the samples.

The *I–V* characteristic curves of PAni nanofibers (Fig. 8) reveal that their conductivities increase with the decrease of interaction between the solvent and aniline. This is attributed to the increase in benzenoid to quinoid ratio,[33] π-stacking of the PAni chains, and density of defect states with the decrease in interaction. The effective conjugation length of PAni nanofibers are thus strongly affected by its conformation because the degree of the *p*-orbital overlap in the extended π-bond is determined by the torsion angle of the backbone.[34] Consequently, the *I–V* measurements corroborate with the FTIR, XRD, and PL results. It has also been observed that the *I–V* curves for the PAni nanofibers were nonlinear, which is supported by the observation of Kaiser et al.[35]. This nonlinearity in the *I–V* characteristic curves of conducting polymers can be explained using an extended fluctuation-induced tunneling and a thermal excitation model. The conductivities of the PAni nanofibers have been found to decrease from P4 to P1 as 3.24×10^{-3}, 1.42×10^{-3}, 9.62×10^{-4}, and 4.62×10^{-4} S/cm, respectively (shown in Table III).

The changes in the structural characteristics of the PAni nanofibers with changing organic solvents of varying solubility parameter are attributed to the intermolecular interactions between the solvent and aniline. When aniline is added to the organic solvents, namely, dichloromethane, 1-butanol, benzene, and carbon tetrachloride, dipole-induced-dipole interactions arise between amino groups of aniline and the solvent. However, dichloromethane and 1-butanol exerts a polar–polar interaction with aniline along with the dipole-induced-dipole interactions. Unlike others, 1-butanol exerts additional hydrogen-bonding interaction with aniline, whereas dichloromethane has the greatest interaction with aniline owing to the smallest difference in the solubility parameter.

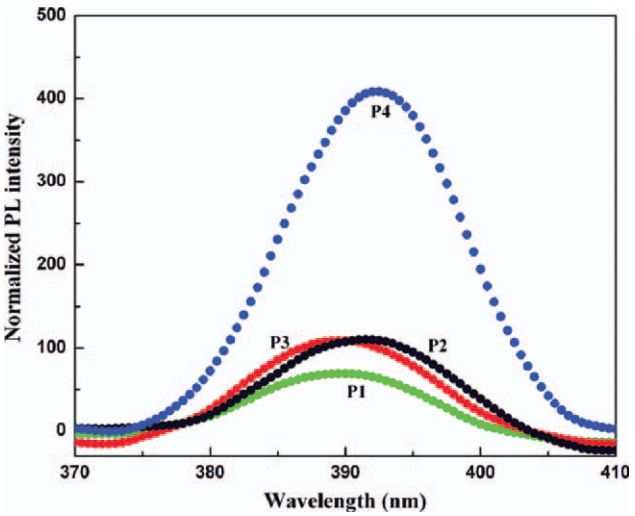

Figure 7 Photoluminescence spectra of P1, P2, P3, and P4 PAni nanofibers. [Color figure can be viewed in the online issue, which is available at wileyonlinelibrary.com.]

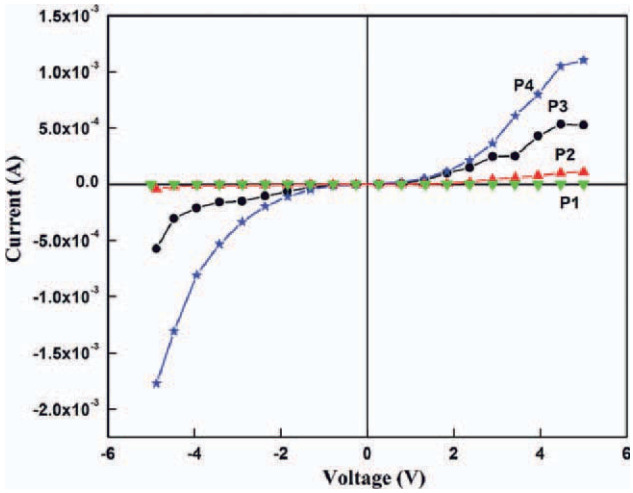

Figure 8 *I–V* characteristic curves of P1, P2, P3, and P4 PAni nanofibers. [Color figure can be viewed in the online issue, which is available at wileyonlinelibrary.com.]

CONCLUSIONS

The difference in the monomer–solvent interaction leads to the variation in the degree of conjugation, domain length, *d*-spacing, and strain as revealed by the various characterization tools. Dipole-induced-dipole, polar–polar, and hydrogen-bonding interaction produced the changes in the internal morphology of PAni nanofibers with the change of organic solvents in the interfacial polymerization technique. This approach of the in-depth study of the interactions between the monomer and the organic solvents would help to precisely control the internal conformations of the PAni nanofibers. Thus, the optoelectronic properties of PAni nanofibers are assertively influenced by the conformation of the polymers.

The authors thank Mr. Rocktotpal Konwarh and Mr. Gautam Das for their valuable inputs during the preparation of the manuscript. Sophisticated Analytical Instruments Facility (SAIF), North-Eastern Hill University (NEHU), Shillong, is acknowledged for TEM imaging.

References

1. Wang, J.; Torardi, C. C.; Duch, M. W. J Synth Met 2007, 157, 851.
2. Wang, C. Y.; Mottaghitalab, V.; Too, C. O.; Spinks, G. M.; Wallace, G. C. J Power Sources 2007, 163, 1105.

3. Li, X. G.; Feng, H.; Huang, M. R.; Gu, G. L.; Moloney, M. G. Anal Chem 2012, 84, 134.
4. Huang, J.; Virji, S.; Weiller, B. H.; Kaner, R. B. Chem Eur J 2004, 10, 1314.
5. Huang, J. Pure Appl Chem 2006, 78, 15.
6. Liu, S.; Wang, L.; Luo, Y.; Tian, J.; Li, H.; Sun, X. Nanoscale 2011, 3, 967.
7. Li, D.; Huang, J.; Kaner, R. B. Acc Chem Res 2009, 42, 135.
8. Li, X. G.; Lu, Q. F.; Huang, M. R. Small 2008, 8, 1201.
9. Saravanan, C.; Palaniappan, S.; Chandezon, F. Mater Lett 2008, 62, 882.
10. Song, G.; Han, J.; Bo, J.; Guo, R. J Mater Sci 2009, 44, 715.
11. Chen, Y. H.; Wu, J. Y.; Chung, Y. C. Biosens Bioelectron 2006, 22, 489.
12. Xing, S.; Zheng, H. e-Polymers 2008, 106, 1.
13. Tran, H. D.; D'Arcy, J. M.; Wang, Y.; Beltramo, P. J.; Strong, V. A.; Kaner, R. B. J Mater Chem 2011, 21, 3534.
14. Anbarasan, R.; Sangeeth, V.; Saravanan, M.; Rajkumar, R.; Anandhaalaguraja, M.; Dhanalakshmi, V. J Macromol Sci B 2011, 50, 704.
15. Jing, X.; Wang, Y.; Wu, D.; Quing, J. Ultrason Sonochem 2007, 14, 75.
16. Li, W. G.; Wang, H. L. J Am Chem Soc 2004, 126, 2278.
17. Zhang, X.; Goux, W. J.; Manohar, S. K. J Am Chem Soc 2004, 126, 4502.
18. Lu, X. W.; Wu, W.; Chen, J. F.; Zhang, P. Y.; Zhao, Y. B. Ind Eng Chem Res 2011, 50, 5589.
19. Huang, J.; Kaner, R. B. J Am Chem Soc 2004, 126, 851.
20. Huang, J. X.; Shabnam, V.; Bruce, H. W.; Richard, B. K. J Am Chem Soc 2003, 125, 314.
21. Yan, W.; Wei, Z. X.; Hsu, C. S.; Wan, M. X. Synth Met 2003, 136, 213.
22. Yangyong, W.; Xinli, J. J Phys Chem B 2008, 112, 1157.
23. Zujovic, Z. D.; Wang, Y.; Bowmaker, G. A.; Kaner, R. B. Macromolecules 2011, 44, 2735.
24. Brandrup, J.; Immergut, E. H.; Grulke, E. A. Polymer Handbook; Wiley: New York, 1999.
25. Huang, J.; Virji, S.; Weiller, B. H.; Kaner, R. B. J Am Chem Soc 2003, 125, 314.
26. Li, X. G.; Huang, M. R.; Duan, W. Chem Rev 2002, 102, 2925.
27. Banerjee, S.; Saikia, J. P.; Kumar, A.; Konwar, B. K. Nanotechnology 2010, 21, 045101.
28. Li, X. G.; Li, A.; Huang, M. R. Chem Eur J 2008, 14, 10309.
29. Jayakannan, M.; Annu, S.; Ramalekshmi, S. J Polym Sci Part B: Polym Phys 2005, 43, 1321.
30. Banerjee, S.; Sarmah, S.; Kumar, A. J Opt 2009, 38, 124.
31. Banerjee, S.; Kumar, A. Nucl Instrum Methods Phys Res Sect B 2010, 268, 2683.
32. Sahu, B. S.; Delachat, F.; Slaoui, A.; Carrada, M.; Ferblantier, G.; Muller, D. Nanoscale Res Lett 2011, 6, 178.
33. Xing, S.; Zheng, H.; Zhao, G. Synth Met 2008, 158, 59.
34. Kim, J. Pure Appl Chem 2002, 74, 2031.
35. Kaiser, A. B.; Park, J. G.; Kim, B.; Lee, S. H.; Park, Y. W. Curr Appl Phys 2004, 4, 497.